



HAL
open science

Gain-scheduled LPV/Hinf controller based on direct yaw moment and active steering for vehicle handling improvements

Moustapha Doumiati, Olivier Sename, John Jairo Martinez Molina, Luc Dugard, Charles Poussot-Vassal

► **To cite this version:**

Moustapha Doumiati, Olivier Sename, John Jairo Martinez Molina, Luc Dugard, Charles Poussot-Vassal. Gain-scheduled LPV/Hinf controller based on direct yaw moment and active steering for vehicle handling improvements. CDC 2010 - 49th IEEE Conference on Decision and Control, Dec 2010, Atlanta, Georgie, United States. pp.6. hal-00536112

HAL Id: hal-00536112

<https://hal.science/hal-00536112>

Submitted on 15 Nov 2010

HAL is a multi-disciplinary open access archive for the deposit and dissemination of scientific research documents, whether they are published or not. The documents may come from teaching and research institutions in France or abroad, or from public or private research centers.

L'archive ouverte pluridisciplinaire **HAL**, est destinée au dépôt et à la diffusion de documents scientifiques de niveau recherche, publiés ou non, émanant des établissements d'enseignement et de recherche français ou étrangers, des laboratoires publics ou privés.

Gain-scheduled LPV/\mathcal{H}_∞ controller based on direct yaw moment and active steering for vehicle handling improvements

M. Doumiati*, O. Sename, J. Martinez, L. Dugard and C. Poussot-Vassal

Abstract—This paper deals with the design of a control scheme that integrates braking and front steering to enhance the vehicle yaw stability and the lateral vehicle dynamics. The proposed VDSC (Vehicle Dynamic Stability Controller) allows control of the yaw rate and obtains good response for the sideslip angle. Besides, this controller takes into account the braking actuator limitations (i.e braking only the rear wheels) and limits the use of the steering actuator only in the linear vehicle handling region (stability region). To reach these objectives, an original parameter dependent LPV controller structure with consistent performance weights is designed. The solution of the problem is obtained within the LMI framework, while warranting \mathcal{H}_∞ performances. To prevent tires longitudinal slip due to brake forces generated by the controller, an ABS strategy is included in the control scheme. Computer simulations, carried out on a complex full vehicle model subject to critical driving situations, confirm the effectiveness of the proposed control system and the overall improvements in vehicle handling and stability.

I. INTRODUCTION

A close examination of accident data reveals that losing the vehicle control is responsible for a huge proportion of car accidents. Under critical driving circumstances, such as emergency cornering, it is usually difficult for a driver to stabilize the vehicle, and dangerous accidents could happen. To ensure vehicle stability and handling, many advanced active chassis control systems based on active yaw moment control have been developed and brought into the market, like the conventional ESP (Electronic Stability program) and the 4WS (4-wheel steering) systems.

Safety of ground vehicles may be greatly improved through active yaw/sideslip control. The basic idea of the active vehicle stability control is to keep the vehicle within the linear or stability region that is familiar to the driver. One approach for yaw and lateral vehicle dynamics improvement is to use differential braking, thereby creating the moment that is necessary to counteract the undesired yaw motion. This technique is referred to as Direct Yaw moment Control (DYC). Some researchers, like in [1] and [2], emphasized the DYC concept to improve the vehicle stability, especially in severe maneuvers. However, this method is not desirable in normal driving situations because of the direct influence of the control action on the longitudinal vehicle dynamics (i.e it causes the vehicle to slow down significantly). An alternative approach is to command additional steering angle to create the counteracting moment. This technique is referred to as Active Steering (AS), and is mainly effective when the

Symbol	Value	Unit	Signification
m	1535	kg	vehicle mass
m_r	648	kg	vehicle rear mass
I_z	2149	kg.m ²	vehicle yaw inertia
C_f	80000	N/rd	Cornering stiffness of front tires
C_r	80000	N/rd	Cornering stiffness of rear tires
l_f	1.4	m	distance COG - front axle
l_r	1	m	distance COG - rear axle
t_r	1.4	m	rear axle length
R	0.3	m	tire radius
μ	[2/5; 1]	—	tire/road contact friction interval
v	[50; 130]	km/h	vehicle velocity interval

TABLE I

NOTATIONS AND VEHICLE PARAMETERS.

lateral tire forces linearly depend on the sideslip angles [3], [4]. AS control collapses when the vehicle reaches the handling limit due to the tire saturations. Consequently, these different control methods are optimized individually in specific handling regions, and the maximum benefit can be gained through the coordinated and combined use of both methods in the control strategy. On this topic, some relevant results in the literature could be found in [5]-[9].

In this paper, a new VDSC (Vehicle Dynamic Stability Controller) system is developed. The proposed VDSC is a unified controller that coordinates AS (for front tires) and DYC in order to preserve the vehicle stability in extreme handling situations, while achieving a good ride comfort. More precisely, this study enhances the existing one proposed by the authors in [10], bringing the following main contributions:

- The VDSC system tracks a desired vehicle behavior, while controlling both the yaw rate and the sideslip angle dynamics.
- Both AS and DYC are activated in the linear region of vehicle handling. However, AS is involved only in a frequency range where the driver is not able to act. Applying this strategy ensures that the added corrective steering angle is not inconvenient for the driver, and that the vehicle speed does not slow down considerably.
- The AS rolls off in severe maneuvers that lead to instability and only DYC (braking only one rear wheel at a time) remains on. The boundary of judging the vehicle stability is deduced from the phase-plane of the sideslip angle and its time derivative.

The proposed VDSC is based on a 2-DOF linear vehicle model and synthesized as a parameter dependent controller, gain-scheduled MIMO (Multi-Input Multi Output) system. This controller activates the required actuator(s) depending on the driving conditions. The overall VDSC is built in the LPV (Linear Parameter Varying) framework with an LMI

M. Doumiati, O. Sename, J. Martinez and L. Dugard are with GIPSA-lab UMR CNRS 5216, Control Systems department, Grenoble INP-ENSE3 University, BP 46, 38402 Saint Martin d'Hères, France *moustapha.doumiati@gmail.com

C. Poussot-Vassal is with ONERA DCSD department, 2 avenue Edouard Belin, 31055 Toulouse, France charles.poussot-vassal@onera.fr

(Linear Matrix Inequalities) solution that warrants the \mathcal{H}_∞ performances.

The response of the vehicle with the proposed control scheme has been evaluated via computer simulations using a full vehicle model validated on a real car.

The rest of this paper is structured as follows. Section II first introduces the global control scheme, and then developed and synthesized the MIMO vehicle dynamical stability controller. Performance analysis is done in Section III through time simulations performed on a complex nonlinear full vehicle model. Conclusions and discussions are given in Section IV.

Paper notations:

Throughout the paper, the following notation will be adopted: index $i = \{f, r\}$ and $j = \{l, r\}$ are used to identify vehicle front, rear and left, right positions respectively. Table I summarizes the notations and values used in the paper.

II. REALIZATION OF THE CONTROL SCHEME

Figure 1 represents the total control scheme. This architecture includes an estimator and a controller. Signals such as steering wheel angle, wheel speeds, yaw rate, lateral acceleration are available in reasonable costs or already exist on vehicle equipped with ESP system. The sideslip angle is a difficult and an expensive measurement to achieve in practice. Thus, it must be estimated. The estimator used here (EKF model-based observer) was proposed by the authors in a previous study [11].

Model-following technique is used in vehicle dynamic control. The yaw rate and the sideslip angle, respectively $\dot{\psi}_d$ and β_d , of a reference model based on the driver's steering input and the vehicle velocity, are the desired responses tracked by the actual vehicle. The reference model is adopted to provide vehicle stability.

As seen in figure 1, both inputs of the proposed controller are the yaw rate and slip angle errors, and the outputs are the active steer angle and the brake torque applied at only one rear wheel at a time depending on the driving situation. It is worthwhile to note that the steering angle applied to the vehicle is $\delta = \delta^d + \delta^+$, where δ^d is the angle provided by the driver and δ^+ is the additive steering angle commanded by the controller and generated by the AS actuator.

In the following, each block of the proposed control system is described in details.

A. Reference model

The aim of the developed VDSC during cornering is twofold: tracking a reference yaw rate and a reference body sideslip angle. In this work, these references values are obtained as the outputs of a 2-DOF (Degree Of Freedom) classical linear bicycle model. The use of this model is explained in detail by Dugoff, Francher, and Segel [12]. Note that roll, pitch, and longitudinal dynamics are neglected to simplify the vehicle dynamics. The equations governing the lateral and yaw motions in this linear model can be expressed as:

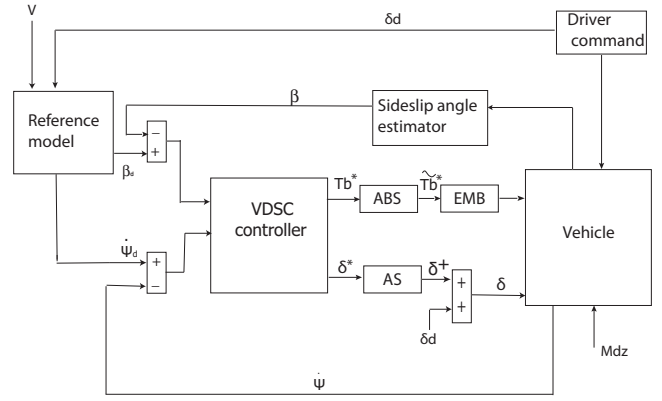


Fig. 1. Global control scheme.

- Equation of lateral motion:

$$mv \left(\dot{\beta} - \dot{\psi} \right) = C_f \left(\delta - \beta - l_f \frac{\dot{\psi}}{v} \right) + C_r \left(-\beta + l_r \frac{\dot{\psi}}{v} \right) \quad (1)$$

- Equation of yaw motion:

$$I_z \ddot{\psi} = C_f \left(-l_f \frac{\dot{\psi}}{v} - \beta - \delta \right) l_f + C_r \left(\beta - l_r \frac{\dot{\psi}}{v} \right) l_r \quad (2)$$

Besides, for a safe drive, these references must be saturated by the physical limit imposed by the current road adhesion coefficient μ . Since the lateral acceleration of the vehicle cannot exceed the maximum friction coefficient μ , the desired yaw rate must be limited by the following value:

$$\left| \dot{\psi}_{max} \right| \leq |\mu g / v| \quad (3)$$

The upper limit β_{max} is obtained by ensuring that the slip angle does not become too large. Thus, the tires are prevented to approach their limits of adhesion. It was found that this upper limit corresponded to $\beta_{max} = \arctan(0.02\mu g)$ (empirical relation). For more details concerning the upper limits formulation, one may refer to [13].

B. VDSC Design

1) Vehicle model for synthesis: The LPV/ \mathcal{H}_∞ controller is obtained based on a linear bicycle model which represents well the lateral and yaw motions of the vehicle (see equations (1) and (2)). However, taking into account the controller structure, the classical bicycle model is extended to include the rear brake torques as inputs:

$$\begin{cases} \dot{\beta} &= (F_{ty_f} + F_{ty_r}) / (mv) + \dot{\psi} \\ \ddot{\psi} &= [l_f F_{ty_f} - l_r F_{ty_r} \\ &\quad - \Delta F_{tx_r} t_r + M_{dz}] / I_z \end{cases} \quad (4)$$

where F_{ty_f} and F_{ty_r} are the front/rear lateral tire forces respectively, ΔF_{tx_r} is the differential rear braking force, which depends on the applied braking torques, and M_{dz} denotes the yaw moment disturbance (i.e effects of the wind, ...). Assuming that low slip value are preserved, ΔF_{tx_r} may be written as:

$$\Delta F_{tx_r} = F_{tx_rl} - F_{tx_rr} \quad (5)$$

$$= \frac{Rm_r g}{2} (T_{brl} - T_{brr}). \quad (6)$$

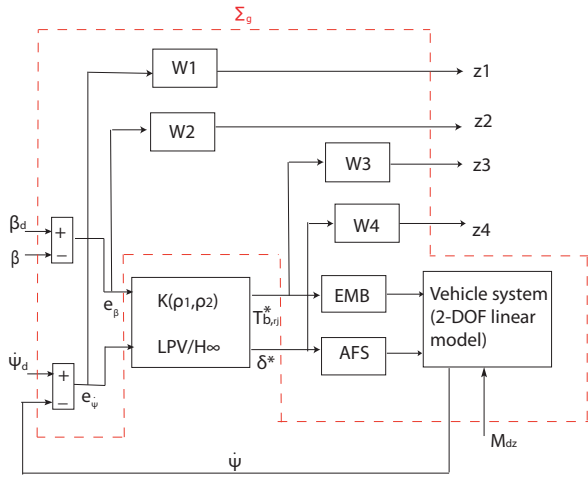


Fig. 2. Generalized plant model.

Consequently, the extended linear bicycle model is given by:

$$\begin{bmatrix} \dot{\beta} \\ \ddot{\psi} \end{bmatrix} = \begin{bmatrix} \frac{-C_f - C_r}{mv} & 1 + \frac{l_r C_r - l_f C_f}{m v^2} \\ \frac{l_r C_r - l_f C_f}{I_z} & \frac{-l_f^2 C_f - l_r^2 C_r}{I_z v} \end{bmatrix} \begin{bmatrix} \beta \\ \dot{\psi} \end{bmatrix} + \begin{bmatrix} \frac{C_f}{l_f C_f} & 0 & 0 & 0 \\ \frac{l_f C_f}{I_z} & \frac{1}{I_z} & a_1 & a_2 \end{bmatrix} \begin{bmatrix} \delta \\ M_{dz} \\ T_{brl} \\ T_{brr} \end{bmatrix} \quad (7)$$

where: $a_1 = -a_2 = \frac{m_r g R l_r}{2 I_z}$.

2) *Generalized plant*: VDSC is the proposed controller that provides the desired braking torque (T_{brj}^*) and the additive steering angle (δ^*) to maintain the vehicle control. VDSC is fed by the yaw rate and sideslip angle errors, $e_{\dot{\psi}}$ and e_{β} respectively, and scheduled by two parameters, ρ_1 and ρ_2 , that evolve according to the driving situations. To synthesize the so called VDSC, the \mathcal{H}_∞ control performance is used. For more information about the \mathcal{H}_∞ and LMI theories, reader can refer to [14], [15]. In the following, we present the generalized synthesis plant, called Σ_g and illustrated in figure 2, together with the performance weighting functions and the actuator dynamics. Σ_g is given thereafter:

$$\Sigma_g : \begin{bmatrix} \dot{x} \\ z \\ y \end{bmatrix} = \begin{bmatrix} A & B_1 & B_2 \\ C_1 & D_{11} & D_{12} \\ C_2 & 0 & 0 \end{bmatrix} \begin{bmatrix} x \\ w \\ u \end{bmatrix} \quad (8)$$

where $w = [\dot{\psi}_d, \beta_d, M_{dz}]^T$ is the exogenous input vector, $u = [\delta^*, T_{brl}^*, T_{brr}^*]^T$ represents the control input signals, $y = [\dot{\psi}, \beta]^T$ is the measurement vector, and $z = [z_1, z_2, z_3, z_4]^T$ contains the weighted controlled outputs which have to be as small as possible.

Weighting functions:

In order to formulate the standard structure for the \mathcal{H}_∞ controller defined in figure 2, the weighting functions W_1 , W_2 , W_3 , and W_4 are defined to characterize the performance objectives and the actuator limitations. The reason behind the weights selection is summarized below:

- z_1 is the weighted yaw rate error output signal. It represents the yaw rate tracking performance. The corresponding weight W_1 is:

$$W_1 = \frac{1}{2G_e} \frac{sG_e/2\pi f_1 + 1}{s/2\pi f_1 + 1} \quad (9)$$

where $f_1 = 1Hz$ is the cut-off frequency of the high pass filter and where $G_e = 0.1$ is the attenuation level for low frequencies ($f < f_1$). In this case 0.1 means that the static error must be lower than 10%.

- z_2 is the weighted sideslip angle error output signal. It represents the sideslip tracking performance. The corresponding weight W_2 is:

$$W_2 = 10^{-4} \frac{1}{2G_e} \frac{sG_e/2\pi f_1 + 1}{s/2\pi f_1 + 1} \quad (10)$$

- z_3 is the braking control signal attenuation. Its associate weight W_3 is:

$$W_3 = 10^{-4} \frac{s/2\pi f_2 + 1}{s/\alpha 2\pi f_2 + 1} \quad (11)$$

where $f_2 = 10Hz$ is the braking actuator bandwidth.

- z_4 is the steering control signal attenuation. Its associate weight W_4 is:

$$W_4 = G_\delta^0 \frac{(s/2\pi f_3 + 1)(s/2\pi f_4 + 1)}{(s/\alpha 2\pi f_4 + 1)^2} \quad (12)$$

$$G_\delta^0 = \frac{1}{(\Delta_f/2\pi f_3 + 1)(\Delta_f/2\pi f_4 + 1)}$$

$$\Delta_f = 2\pi(f_4 + f_3)/2$$

where $f_3 = 1Hz$ is lower limit of the actuator intervention and $f_4 = 10Hz$ is the steering actuator bandwidth. This filter is designed in order to allow the steering system to act only in $[f_3, f_4]$ frequency range. Outside of this frequency range, the filter rolls off. Between the frequency, and more specifically, at $\Delta_f/2$, the filter gain is unitary. This filter design is inspired from [3].

These weighting functions are recalled in the sensitivity function plots as upper bounds limits, $1/W_i$ (see figure 3). More details are provided in the next subsection.

3) *LPV controller structure and LMI solution*: The controller structure is fixed, but we introduce two parameters dependency, ρ_1 and ρ_2 , on the control output matrix. The controller has the following structure:

$$K(\rho) : \begin{cases} \dot{x}_c = A_c(\rho_1, \rho_2)x_c + B_c(\rho_1, \rho_2)e_{\dot{\psi}} \\ \begin{bmatrix} \delta^* \\ T_{brl}^* \\ T_{brr}^* \end{bmatrix} = \underbrace{\begin{bmatrix} \rho_1 & 0 & 0 \\ 0 & \rho_2 & 0 \\ 0 & 0 & 1 - \rho_2 \end{bmatrix}}_{C_c(\rho_1, \rho_2)} C_c^0(\rho_1, \rho_2)x_c \end{cases} \quad (13)$$

Consequently, according to ρ_1 and ρ_2 dependency parameters, a particular controller output will be used. More specifically:

- Steering action is used only if the vehicle is in the stability region. The boundary for judging the vehicle stability is derived from the phase plane of the sideslip angle and its time derivative. A stability bound defined in [8] is used here, which is formulated as:

$$SI < 0.8. \quad (14)$$

where $SI = \left| 2.49\dot{\beta} + 9.55\beta \right|$ is the "Stability Index". Thus, ρ_1 is chosen as:

$$\rho_1 = \begin{cases} 1 & \text{if } SI < 0.8 \\ 0 & \text{if } SI > 0.8 \end{cases} \quad (15)$$

- The braking torque generated by the controller is always positive and is applied at one wheel at each time. It is worthwhile to note that, besides its effectiveness in generating a yaw moment, another advantage of the scheme to apply the brake torque only at one wheel at each time is that the vehicle is not so much decelerated as when brake torque is applied at more than one wheel to generate the same amount of yaw moment. Consequently:

- when $\rho_2 = 1$, the $T_{b_{rr}}^*$ signal is set to zero
- when $\rho_2 = 0$, the $T_{b_{rl}}^*$ signal is set to zero

Then, by choosing:

$$\rho_2 = \text{sat}_{[0,1]}[\text{sign}(e_{\dot{\psi}})] \quad (16)$$

when we have,

$$\begin{aligned} e_{\dot{\psi}} > 0 &\Rightarrow \rho_2 = 1 \text{ (only rear left brake is activated)} \\ e_{\dot{\psi}} \leq 0 &\Rightarrow \rho_2 = 0 \text{ (only rear right brake is activated)} \end{aligned} \quad (17)$$

which is consistent with the braking torques practical behavior ($\dot{\psi} > 0$ in the counterclockwise direction).

The interest of this original LPV structure is that during the synthesis step, the controller knows which actuator(s) to activate at each time.

Considering the structure discussed above, it is obvious that the system model and actuators are LTI, but the controller is LPV. The stabilizing controller, ensuring \mathcal{H}_∞ performances while minimizing the attenuation level γ for $\rho_1 \in \{0, 1\}$ and $\rho_2 \in \{0, 1\}$, is obtained using the LMI tools. The polytopic approach to this problem consists on finding a solution at each vertex of the polytope described by $\rho_i = [\rho_1, \rho_2, 1 - \rho_2]$, by using a common Lyapunov function. For more details on the computation solution, reader is invited to read [10] and [15]. By solving the LMI problem using Yalmip interface [16] and SeDumi solver [17], one obtains the suboptimal value $\gamma_{opt} = 1.0669$.

Remark: It is crucial to note that an LTI controller structure synthesized on the same plant Σ_g with the same weighted filters, results in a controller which may provide a negative torque (equivalent to an acceleration), which is, practically impossible [10].

According to the sensitivity functions Bode diagrams illustrated in figure 3, it is interesting to make the following deductions:

- The yaw rate error signal, $e_{\dot{\psi}}$, is well attenuated for the LPV controller (see figure 3(a)).
- The sideslip angle error, e_β , is not attenuated so much. However, we note that thanks to the LPV design the closed-loop stability of the system is ensured, and the sideslip angle is supposed to follow its target (see figure 3(b)).

- Figure 3(c) shows that if the steering is activated ($\rho_1 = 1$), it decreases the use of braking for controlling the yaw rate.
- For the LPV control strategy, when the steering control is activated ($\rho_1 = 1$), it acts on the specified frequency range as illustrated in figure 3(d). Moreover, this figure elucidates the contribution of the steering in controlling the yaw rate. For $\rho_1 = 0$, steering is forbidden.

C. ABS

To prevent tires longitudinal slip due to brake forces generated by the controller, an ABS strategy is included in the control scheme. The local ABS is implemented on each of the rear wheels, and it is activated only when high slipping occurs. It provides $\widetilde{T}_{b_{rj}}^*$, the braking torque, according to the set point $T_{b_{rj}}^*$ provided by the VDSC control bloc (see figure 2). This ABS system is recently developed in [18].

D. Actuator models

The control input signals used are the steering angle and the rear braking torques. Let consider the following actuators:

- As braking system, we consider an EMB (Electro Mechanical Braking) actuators, providing a continuously variable braking torque. The model is given by:

$$\dot{T}_{b_{rj}} = 2\pi\varpi(\widetilde{T}_{b_{rj}}^* - T_{b_{rj}}) \quad (18)$$

where, $\varpi = 10\text{Hz}$ is the actuator cut-off frequency, $\widetilde{T}_{b_{rj}}^*$ and $T_{b_{rj}}$ are the local braking controller and actuator outputs respectively. Note that in this paper, only the rear braking system is used to avoid coupling phenomena occurring with the steering system. This actuator control is limited between $[0, 1200]$ Nm.

- As Active Steering (AS) system, we consider an active actuator providing an additional steering angle. Such actuator is modeled as:

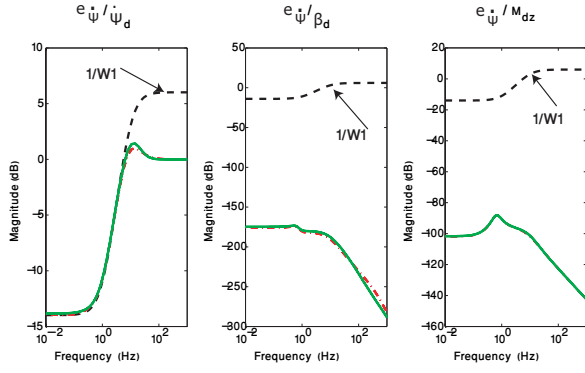
$$\dot{\delta}^+ = 2\pi\kappa(\delta^* - \delta^+) \quad (19)$$

where, $\kappa = 10\text{Hz}$ is the actuator cut-off frequency, δ^* and δ^+ are the steering controller and actuator outputs respectively.

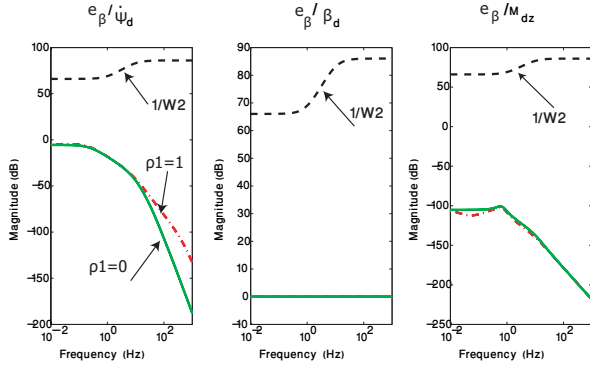
III. SIMULATIONS

Simulations from nominal as well as adverse driving conditions were carried out on different road conditions in order to assess the performance of the proposed control scheme. Simulations are performed using a full vehicle model validated on a real french car: (*Renault Mégane Coupé*). In this paper, we report a double-lane-change maneuver on a dry road maneuver (one of a number of simulations that we carried out), where the dynamic contributions play an important role. In the following, on each plot, the uncontrolled 'Mégane' is plotted in blue dot, the 'LPV' control in red dashed and the yaw rate and sideslip angle references in black solid.

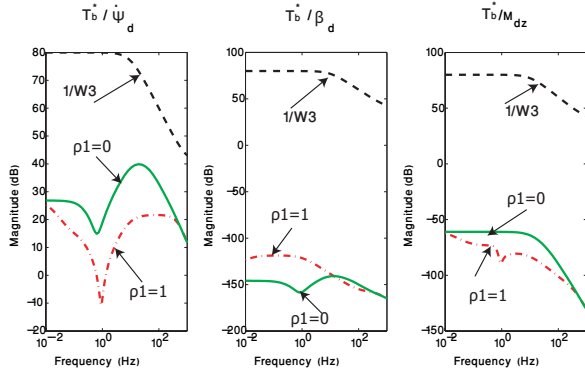
Scenario description: In this critical test, the vehicle is driven at very high speed 150 km/h . The yaw rate, the sideslip angle, and the trajectory of the vehicle are shown in figure 4. Figure 4 confirms that the vehicle with the proposed control task is superior to the uncontrolled vehicle in terms



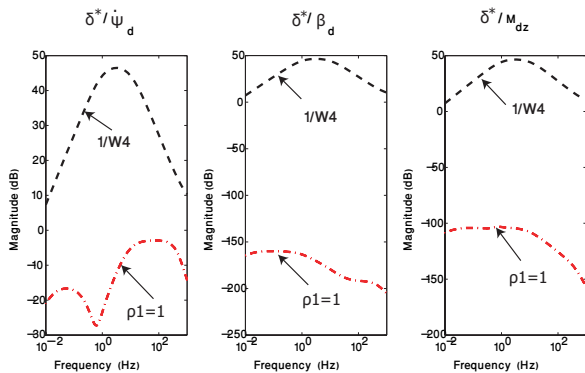
(a) Closed loop transfer functions between $e_{\dot{\psi}}$ and exogenous inputs.



(b) Closed loop transfer functions between e_{β} and exogenous inputs.



(c) Closed loop transfer functions between T_b^* and exogenous inputs.



(d) Closed loop transfer functions between δ^* and exogenous inputs.

Fig. 3. Closed loop transfer functions: LPV (red dashed ($\rho_1 = 1$), or green solid ($\rho_1 = 0$)) synthesis results; Weighting functions (black dashed) of $1/W_1$, $1/W_2$, $1/W_3$, and $1/W_4$.

of following the linear model behavior. The sideslip angle of the controlled vehicle remains close to its target all over the vehicle trajectory, which ensures the vehicle stability. Figure 5(a) shows the generated corrective steering angle and the brake torques to enhance the lateral vehicle control. It is obvious that the LPV/\mathcal{H}_∞ controller only provides positive braking torques, which are achievable by the considered actuators. Therefore, the controller fits to the actuator constraints. For this test, due to braking, the vehicle speed is reduced to 145 km/h , which is not much compared to 150 km/h . Figure 5(b) illustrates how the stability index and the dependency parameters ρ_1 and ρ_2 evolve according to the driving situations:

- $\rho_1 = 1$ ($SI < 0.8$) \rightarrow Steering is activated.
- $\rho_2 = 1$ ($e_{\dot{\psi}} > 0$) \rightarrow Left brake is activated, otherwise, the right brake is activated.

Note that, even when scheduling, the closed-loop stability of the system is ensured thanks to the LPV design.

IV. CONCLUSION

Vehicle handling and stability can be effectively improved using steering and braking systems, a new LPV/\mathcal{H}_∞ controller, that coordinates between these two actuators, is designed in this paper. The proposed LPV controller is designed in an original way and ensures that:

- The steering action is activated only in normal driving condition, and in a specified range of frequency where the driver could not act.
- The braking torque is always positive by selecting the appropriate rear wheel.

Since, the general structure of the proposed control scheme does not involve any online optimization process, it shows to be easy to function in real-time.

Simulation of a critical driving situations that compare the responses of a controlled vehicle with respect to a passive vehicle show the validation of the proposed control design. Future work consists to implement the controller on a real car, and to test its robustness with respect to real driving conditions.

REFERENCES

- [1] J. H. Park, H_∞ direct yaw-moment control with brakes for robust performance and stability of vehicles, JSME International Journal, Series C, Vol. 44, No. 2, 2001
- [2] M. Canale, L. Fagiano, M. Milanese, and P. Borodani, Robust vehicle yaw control using an active differential and IMC techniques, Control Engineering Practice, Vol. 15, pages 923-941, 2007.
- [3] B. A. Guven, T. Bunte, D. Odenthal, and L. Guven, Robust two degree-of-freedom vehicle steering controller design, IEEE Transaction on Control System Technology, Vol. 15, pages 554-565, 2007.
- [4] S. Mammari and D. Koenig, Vehicle handling improvement by active steering, Vehicle System Dynamics, Vol. 38, No. 3, pages 211-242, 2002.
- [5] M. Nagai, Y. Hirano, and S. Yamanaka, Integrated control of active rear wheel steering and direct yaw moment control, Vehicle System Dynamics, Vol. 27, pages 357-370, 1997.
- [6] B. L. Boada, M. J. L. Boada, and V. Diaz, Fuzzy-logic applied to yaw moment control for vehicle stability, Vehicle System Dynamics, Vol. 43, No. 10, pages 753-770, 2005.
- [7] G. Burgio and P. Zegelaar, Integrated vehicle control using steering and brakes, International Journal of Control, Vol. 79, No. 5, pages 534-541, 2006.
- [8] J. He, D. A. Crolla, M. C. Levesley, and W.J. Manning, Coordination of active steering, driveline, and braking for integrated vehicle dynamics control, Proc. IMechE, Vol. 220, PartD: Automobile Engineering, 2006.

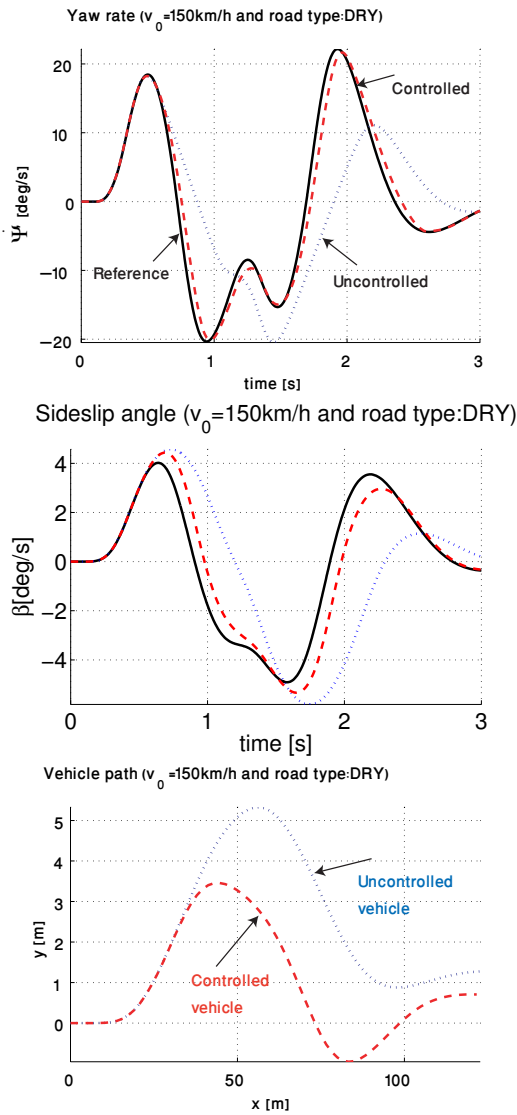
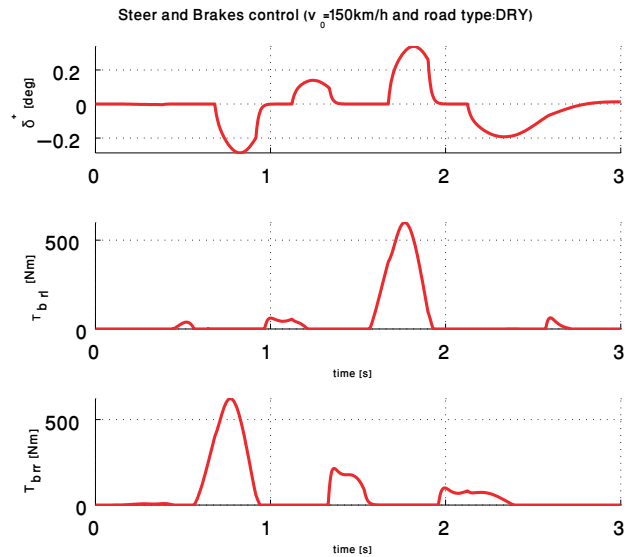
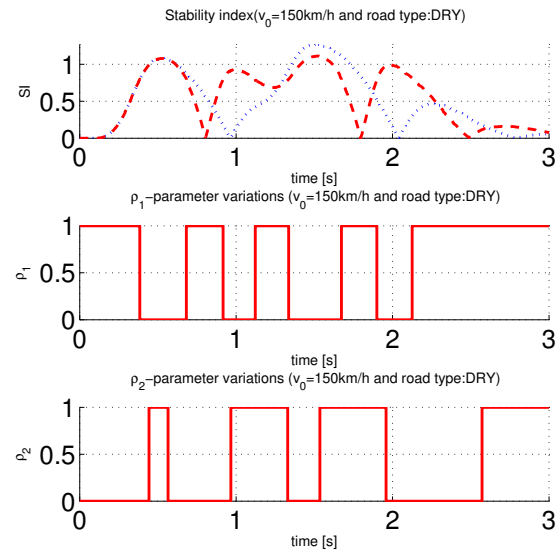


Fig. 4. Vehicle responses in a double lane change maneuver (dry road): with LPV (red dashed), Uncontrolled (blue dot), Reference model (black solid)



(a) Control signals for the double lane change maneuver.



(b) ρ_1 and ρ_2 variations: $\rho_1 = 1 \rightarrow$ Steering is activated, $\rho_2 = 1 \rightarrow$ Left brake torque is activated, otherwise, right brake torque is activated.

- [9] X. Yang, Z. Wang, and W. Peng, *Coordinated control of AFS and DYC for vehicle handling and stability based on optimal guaranteed cost theory*, Vehicle System Dynamics, Vol. 47, No. 1, pages 57-79, 2009.
- [10] C. Poussot-Vassal, O. Sename, and L. Dugard, *Robust vehicle dynamic stability controller involving steering and braking*, Proceedings of the European Control Conference, Budapest, Hungary, 2009.
- [11] M. Doumiati, A. Victorino, A. Charara, and D. Lechner, *A method to estimate the lateral tire force and the sideslip angle of a vehicle: Experimental validation*, Proceedings of the American Control Conference, Baltimore, USA, 2010.
- [12] H. Dugoff, P.S. Francher, and L. Segel, *An analysis of tire traction properties and their influence on vehicle dynamic performance*, SAE transactions, vol. 79, pp. 341-366, 1970.
- [13] R. Rajamani, *Vehicle dynamics and control*, Springer, 2006.
- [14] S. Skogestad and I. Postlethwaite, *Multivariable feedback control, analysis and design*, Wiley, 2007.
- [15] C. Scherer, P. Gahinet, and M. Chilali, *Multiobjective output-feedback control via LMI optimization*, IEEE Transaction on Automatic Control, Vol. 40, pages 896-911, 1997.
- [16] J. Lofberg, *YALMIP: a toolbox for modeling and optimization in MATLAB*, Proceedings of the CACSD Conference, Taipei, Taiwan, 2004.
- [17] J. F. Sturm, *Using seDuMi 1.02, a Matlab toolbox for optimization over*

- symmetric cones*, Optimization Methods and Software 11-12, pages 625-653, Special issue on Interior Point Methods, 1999.
- [18] M. Tanelli, R. Sartori, and S. Savaresi, *Combining Slip and deceleration control for brake-by-wire control systems: a sliding-mode approach*, European Journal of Control, Vol. 13, pages 593-611, 2007.
- [19] P. Apkarian and P. Gahinet, *A convex characterization of gain scheduled H_∞ controllers*, IEEE Transaction on Automatic Control, Vol. 40, pages 853-864, 1995.

Fig. 5. Control signals according to ρ_1 and ρ_2 variations.